Journal of Structural Geology 31 (2009) 288–300

Contents lists available at ScienceDirect

Journal of Structural Geology

journal homepage: www.elsevier.com/locate/jsg

Mechanisms of faulting and permeability enhancement during epithermal mineralisation: Cracow goldfield, Australia

Steven Micklethwaite*

Research School of Earth Sciences, The Australian National University, Canberra, ACT 0200, Australia

ARTICLE INFO

Article history:
Received 16 May 2008
Received in revised form
13 November 2008
Accepted 24 November 2008
Available online 13 December 2008

Keywords:
Permeability
Veins
Dilatant faults
Mineralisation
Epithermal
Kinematics

ABSTRACT

The geometries, kinematics, and failure mechanisms of epithermal fault-vein networks are examined at the Cracow goldfield, Queensland, Australia, and compared with observations of active geothermal areas. Quartz–carbonate cementation and precious metal mineralisation is confined to a network of steeply dipping faults (>70°). Breccia textures indicate fault rock formed from repeated events, involving large components of dilation during fracture, wall-rock fragmentation, and mineral precipitation. New fault rock tended to form on the margins of pre-existing fault rock, generating thick zones up to 10 m wide (fault cores) and accumulating up to 300 m normal offsets. The fault-vein networks are segmented, corrugated over tens of metres along strike, and contain complex fracture networks in step-over zones. Mineralisation is not associated with any specific fault location, but occurs along planar segments of faults, in step-over zones, at fault tips and where fault dips change. The wall rocks surrounding the faults contain networks of shear and extension veins, with a large range of orientations. Furthermore, kinematic indicators on the faults are broadly normal dip-slip, but vary to oblique and strike-slip with no obvious relationship to geometry or location along the fault. Inconsistent fault kinematics and the range of wall rock vein orientations are attributed to transient changes in stress state, due to intrusion of nearby dykes. As a result, permeability would have been enhanced by dilatancy in fault rock and wall rock fractures, when corrugated normal faults temporarily failed in oblique or strike-slip events. Other permeability enhancement mechanisms likely included failure driven by high fluid pressures, and failure where faults steepen (near the Earth's surface or at jogs). Mineralisation was associated with repeated, transient pulses of fluid flow rather than a steady-state process.

1. Introduction

Processes operating in geothermal environments are responsible for the development of epithermal mineralisation (e.g. White, 1955, 1981; Henley, 1985; Simmons and Browne, 2000; Simmons et al., 2006), and active faulting in these environments likely results in the formation of fault-vein hosted, gold deposits. Geophysical observations demonstrate that geothermal environments can be remarkably dynamic due to interactions between faulting, intrusive activity and elevated pore fluid pressures (Hill, 1977; Hill et al., 1993; Dreger et al., 2000; Waite and Smith, 2002), thus structural behaviour and fluid flow may be strongly influenced by this coupling. Nevertheless, although epithermal deposits are well understood from a geochemical perspective (Simmons et al., 2006), very little is known about the growth, failure mechanics and permeability enhancement processes of epithermal fault-vein networks. This is despite the observation that epithermal structures display some unusual characteristics, such as large amounts of dilatancy, steep dips and kinematics that are enigmatic or difficult to determine (e.g. Brathwaite and McKay, 1983; Nortje et al., 2006).

Fluid flow in fault systems has been studied from mechanical and geometric perspectives. Simple geometric models suggest fault terminations, or linkages between fault segments, are domains of high fracture density and connectivity, and are therefore likely to localise fluid flow (Hancock et al., 1999; Cox et al., 2001; Rowland and Sibson, 2004; Cox, 2005). Rifting associated with geothermal environments tends to be dominated by normal dip-slip faulting (e.g. Rowland and Sibson, 2001). Because normal fault segments link and generate fracturing down-dip through jogs, and along-strike through relay zones, permeability enhancement is predicted horizontally and vertically around the perimeter of fault segments, depending on the direction of fluid flow relative to the orientation of the fault plane. Curewitz and Karson (1997) inferred that

* Correspondence to present address: CODES, School of Earth Sciences, University of Tasmania, Private Bag 126, Hobart, TAS 7001, Australia. Tel.: +61 2 6125 5169; fax: +61 2 6251 8253.
E-mail address: steven.micklethwaite@utas.edu.au

0191-8141/$ – see front matter © 2008 Elsevier Ltd. All rights reserved.
doi:10.1016/j.jsg.2008.11.016

fracture-related permeability in these fault locations is maintained, due to stress concentrations arising from fault propagation and interaction. Other studies emphasise that permeability can be enhanced along fault segments, not just step-over and linkage domains, because dense networks of fractures and subsidiary faults also develop in the wall-rocks to a fault core (Caine et al., 1996; Evans et al., 1997; Shipton et al., 2005). Fault cores themselves can be barriers or conduits to fluid flow (Rowland and Sibson, 2004), and there is strong along-strike spatial variation in the hydraulic configuration of faults, as indicated by surface temperature measurements of normal faults associated with geothermal fluids (Fairley and Hinds, 2004; Heffner and Fairley, 2006). Relevant to this, drilling of active fault systems demonstrated that a small percentage of fault-related fractures, which are well oriented for the regional stress regime, maintains the largest hydraulic conductivities (Barton et al., 1995; Davatzes and Hickman, 2005).

Experimental studies have shown fault-fracture networks are rapidly cemented in structurally controlled hydrothermal environments (Brantley, 1992; Tenthorey et al., 2003; Tenthorey and Fitz Gerald, 2006), suggesting repeated slip events are required to explain the multiple increments of opening and slip observed in cemented fault breccias (Woodcock et al., 2007). Fault-slip permeability enhancement processes may be fluid-pressure dependent or stress dependent in environments relevant to epithermal deposits. Firstly, in some circumstances overpressuring of fluids within compartments in the crust triggers fault rupture and induces transient permeability along fault planes or associated fracture networks (Rowland and Sibson, 2004; Cox, 2005; Davatzes and Hickman, 2005; Talwani et al., 2007). Secondly, fault ruptures generate coseismic static stress changes, which have been related to changes in permeability and fluid flow around fault systems (Muir-Wood and King, 1993; Micklethwaite and Cox, 2004, 2006). Coseismic static stress changes are small but they correlate with domains of time-dependent damage, such as the locations of aftershocks, and are likely to be domains of large, fracture-related fluid flux (Sheldon and Micklethwaite, 2007). These studies indicate that the dynamic behaviour of faulting and veining—the rapid creation then loss of fracture permeability—is an important issue to address in the shallow-level, hard-rock, hydrothermal environments of epithermal deposits.

The objective of this study is to provide a comprehensive structural description of the geometry, dimensions, macroscopic deformation mechanisms and displacement characteristics of a well-constrained epithermal fault-vein network; the Cracow goldfield, in South East Queensland (Fig. 1). Particular attention is paid to the kinematics of the system. Observations are related to fault mechanics, especially fault behaviour in geothermal areas, and implications are explored for processes of permeability enhancement and fluid flow. Surface mapping, drillcore logging, underground exposures and geophysical datasets (ground- and heli-magnetic data), supplied by Newcrest mining company, were used to constrain the fault systems and associated dyke networks.

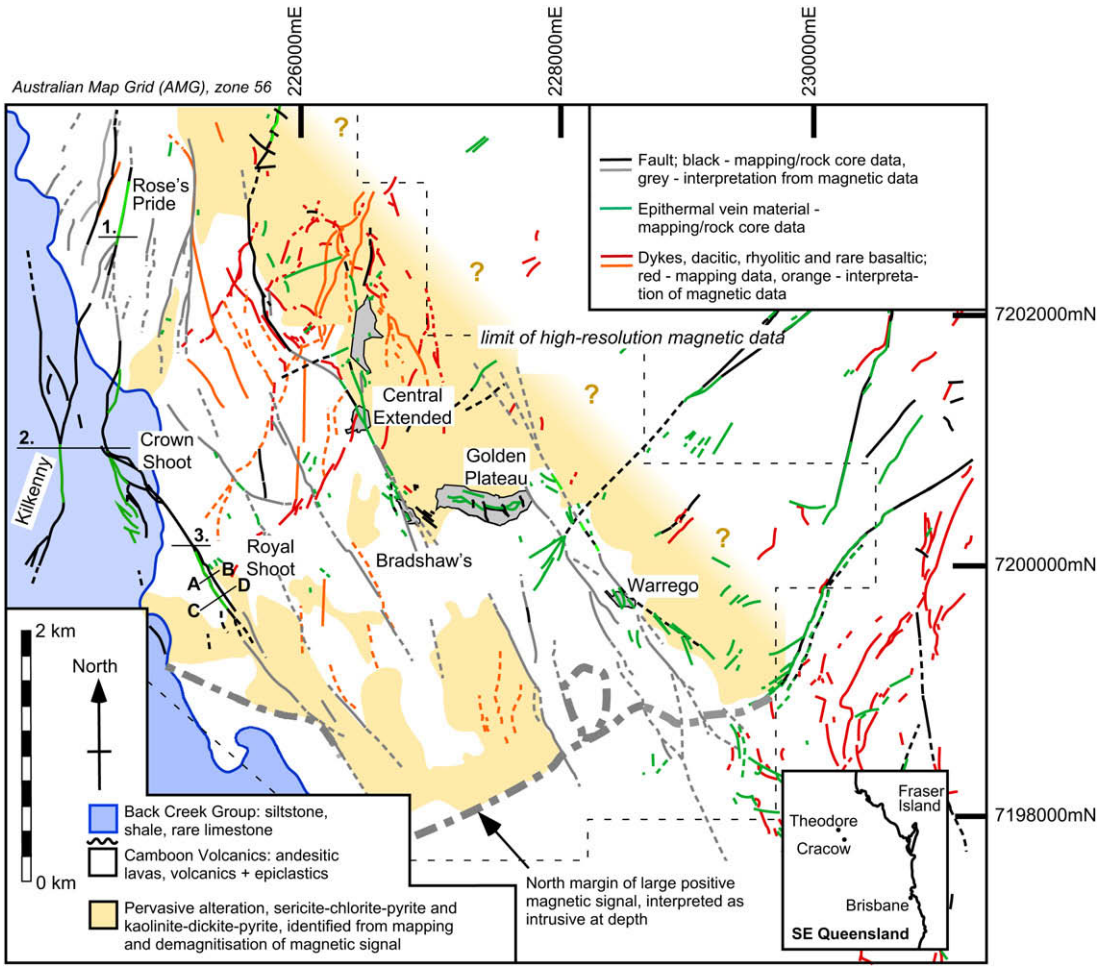

Fig. 1. Geology of the Cracow goldfield, showing the structural patterns of faults, veins and dykes, the distribution of alteration and the locations of the cross-sections shown in Figs. 3 and 4. Pit outlines are given by the grey polygons. Inset map provides the location of Cracow in South East Queensland.

2. Cracow's epithermal fault system

The Cracow goldfield (Worsley and Golding, 1990; Braund, 2006) is located in Queensland, Australia, approximately 350 km northwest of Brisbane. The goldfield is hosted in rocks of the Camboon Volcanics on the western margin of the New England Orogeny, which was part of a convergent continental margin active over an extensive period of time, from the Cambrian to Carboniferous (Holcombe et al., 1997). Western sections of the goldfield subcrop beneath overlying sediments of the large Bowen Basin (Fig. 1), whereas 6 km to the east, Camboon Volcanics are unconformable on the Tordsdale Beds (rhyolitic tuffs and flows).

Camboon Volcanics in the Cracow area are composed of andesite–trachyandesite volcanics, plus lesser volcaniclastic and fine-grained epiclastic units, dipping 15–20° southwest (Jones et al., 1996). Volcaniclastic and epiclastic units act as stratigraphic markers across Cracow's faults, although caution is required because these units are not continuous and vary in thickness dramatically along strike. K–Ar ages of horneblende and plagioclase, near the base of the Camboon Volcanics and at its top respectively, indicate volcanism between ~312 and 283 Ma (Jones et al., 1996). However, problems have been noted with resetting of K–Ar ages in the New England Orogen (Allen, 2000).

Basalt and rhyodacite-dacite dykes plus some diorite bodies intrude the sequence. The rhyodacite dykes are interpreted to be synchronous with Cracow's epithermal fault-vein system because some dykes contain epithermal vein fragments whereas other dykes are affected by the alteration associated with the epithermal veins. One dyke was dated with a U–Pb zircon method at 291.1 ± 5.3 Ma (reported in Dong and Zhou, 1996), which therefore constrains the timing of mineralisation. Further north in the New England Orogen, rhyolitic and dacitic dykes with similar strike orientations yield a SHRIMP zircon age of ~284 Ma (Allen et al., 1998). The mafic dykes intrude basal units of the overlying Bowen Basin sediments and crosscut mineralised veins, and have been interpreted to have a later Triassic age. The time period for mineralisation at Cracow appears to coincide with back-arc extension in the region. Back-arc extension was interpreted on the basis of silicic magmatism and sedimentation, plus distinct changes in the petrography, composition and isotopic ratios of dykes (Holcombe et al., 1997; Allen, 2000). Dyke intrusion plus mineralisation appear to have occurred not long after deposition of the host rocks.

No sinters have been drilled or mapped in the area, and epithermal mineralisation is known to go to depths of at least 500 m beneath the present day surface (Braund, 2006), raising questions as to what the original formation depth was for mineralisation. The host rocks are dominated by massive andesitic volcanic rocks and mineralisation is restricted to quartz–carbonate+/−adularia fault breccias and veins. This is a significant observation because it implies matrix permeability was small and fluid flow was predisposed to be fracture dominated and structurally controlled during mineralisation (Rowland and Sibson, 2004).

2.1. Characteristics of the fault system

Cracow's epithermal structures are referred to as faults because they are discontinuities containing a finite thickness of cemented fault rock (gouge, breccia etc.) across which there is a significant shear displacement, as will be demonstrated below. These structures also record metre-scale components of dilatancy, cemented by quartz–carbonate (qz-carb), and their formation likely involved increments of extensional-shear. To describe the fault systems at Cracow, it is useful to revisit terminology associated with fault systems (Fig. 2) because this terminology has not previously been applied to mineralised epithermal environments.

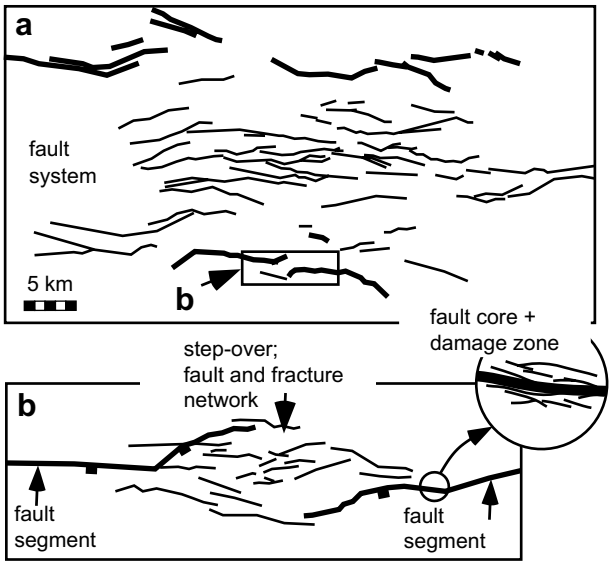

Fig. 2. Terminology of features commonly observed in fault systems.

Fault systems are composed of multiple linked and unlinked faults of differing dimensions and displacements, which relate to one another kinematically and spatially (Walsh and Watterson, 1991). Faults within a system tend to be segmented. When along-strike displacement data is available *fault segments* correspond to maxima in fault displacement, whereas zones between segments correspond to displacement minima (Peacock and Sanderson, 1991; Bull et al., 2006) and this segmentation can occur at a variety of scales (Soliva and Benedicto, 2004). However, in detail, zones between segments correspond with complex fracture/fault networks or bedding rotation, and when this second-order strain is accounted for few real displacement minima exist (Walsh et al., 2003). Segmentation can arise from the linkage of previously separate faults, either along-strike or down-dip (Cowie, 1998; Soliva and Benedicto, 2004), or where a single fault surface at depth develops into an array of fault surfaces (Walsh et al., 2003). In the absence of along-strike displacement data the lengths of fault segments are approximated from Fig. 1, by measuring the relatively continuous/planar sections of a fault often linked to other continuous/planar sections across step-overs or zones of complexity. *Fault step-overs* are unlinked or linked areas between the tips of neighbouring en echelon fault segments. In this paper *fault jogs* refer to hard-linked changes in geometry down the dip of a fault, whereas *step-overs* refer to along-strike changes in geometry associated with complex fault-vein networks between fault segments. Normal fault jogs are contractional or extensional depending on the stepping direction of the jog relative to the slip movement on the fault.

An approximately linear relationship exists between maximum fault displacement and length for normal fault populations (Cowie and Scholz, 1992; Gillespie et al., 1992; Dawers et al., 1993; Schlische et al., 1996; Bailey et al., 2005), although it is not clear if this relationship holds for fault growth in magma assisted rifts (see Rowland et al., 2007). It is also common to observe that where the displacement on one fault decreases, and the fault terminates, new faults begin along-strike with a step-over zone of structural complexity in-between (Fig. 2). Indeed, when the displacement of normal faults is summed perpendicular to fault strike, in serial transects across a rift, the transects describe constant aggregate displacement along the strike of the rift (Walsh and Watterson, 1991; Bull et al., 2005; Nicol et al., 2006). Taken together, these observations suggest fault systems are kinematically coherent and

exhibit some systematic behaviour with regards to their nucleation, growth and development.

At Cracow, two mineralised fault sets are present based on orientation of their strikes and their distribution—one strikes N–S to NW–SE and hosts the majority of gold mineralisation in the Cracow area, a second system with minor historic mineralisation (striking NE–SW) is located on the eastern side of the area. No reliable crosscutting relationships are observed between the two fault sets (Fig. 1). From this point on, only the characteristics and rock types of the first fault system (N–S to NW–SE strike) are considered.

Gold mineralisation is clearly hosted in qz-carb veins and cemented fault-breccias but only a small percentage contains economic gold resources relative to the total population of mapped epithermal veins. On the kilometre scale, mineralised faults are broadly located at the margins of domains of pervasive clay-rich alteration, but this relationship is not understood and underground exposures on the metre scale, adjacent to the faults, can appear to be remarkably unaltered. Faults and veins of a range of different lengths are identifiable and mineralised (Figs. 1 and 3), but it is the larger faults that host economic grade mineralisation, such as the Kilkenny, Royal-Rose and Golden Plateau faults (4–7 km long; Fig. 1), whereas structures <1 km in length are uneconomic.

There is also a systematic pattern to the spacing between faults, with smaller faults or fault segments (i.e. segments ≤ 1.5 km in length) being more closely spaced than larger faults (Fig. 3). In the southern part of the area (Fig. 1) an apparent paucity of faulting is likely due to lack of data arising from diminished magnetic signal, a lack of exploration drilling and thick alluvium cover. The faults bifurcate from north to south along-strike. Fault tip branching and hard-linked step-overs are common features between segments. Segment lengths of $\sim$1–1.5 km link to form larger through-going structures, whose final length is uncertain but is a minimum of 7 km (e.g. Royal-Rose fault). At smaller scales, Cracow's faults are corrugated along their strike, with wavelengths of tens of metres and amplitudes of 1–3 m. The corrugations are parallel with the dip of the fault plane and their dimensions are subtle relative to the kilometre-scale lengths of the faults.

A critical observation is that epithermal vein/breccia material is not continuous along the strike or down the dip of a structure, even when the geometry of the structure does not change (Figs. 1 and 4). Mapping and drill core data show that the along-strike and down dip continuation of veins or cemented breccias are domains of gouge, shearing, thin veining and clay alteration; indicating the structures are continuous but with distinct changes in the type of fault rock comprising the structure. Furthermore, epithermal veins and mineralisation are not exclusive to step-over zones or any specific fault location. In map view, veins are located at fault tips (Bradshaws pit), fault splays (Central Extended pit), as well as along relatively planar fault segments (Royal underground mine). Mineralisation broadly correlates with the thickening of lodes and in cross section thickening can be found where the faults steepen, where they shallow, and also along planar sections of the faults (Fig. 4). At the Royal deposit, lode thickness has some correlation with changes in dip where the structure steepens (as would be expected for normal dip-slip on the structures), however thick vein material also occurs along less steeply dipping relatively planar sections of the fault. The Kilkenny and Crown structures (Fig. 4) show the dip of the lodes varying from 70° to 90°, with thickening in fault-vein cores developed along subvertical planar sections of the Crown structure, and thickening on the Kilkenny structure where normal dip-slip ought to have produced thinning (a contractional bend). These observations suggest fault core thickness is not solely controlled by fault geometry.

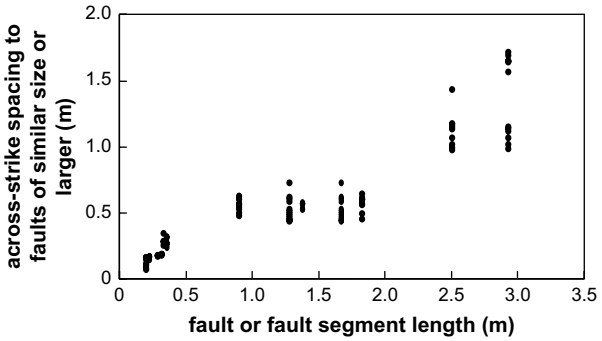

Fig. 3. Across-strike spacing versus fault/fault segment length. Measurements from the NW quarter of Fig. 1, where map data was considered to be well-constrained by field mapping, drill-core intersections and magnetic data. Results should be viewed as semi-quantitative because, in the absence of along-strike displacement profiles, fault segment lengths were interpreted only on the basis of geometry.

Stratigraphic normal dip-slip offsets of 100 m to 300 m have been measured across the Royal-Rose fault, using drillcore data. For example, Fig. 5 shows that coarse grained volcaniclastic units, correlated across the Royal lode, have normal dip-slip offsets of 230 m and 245 m. It is possible the volcaniclastic units either side of the Royal-Rose fault are not the same, in which case a minimum offset of $>$300 m exists, because this implies the correlative unit has been eroded away in the footwall of the Royal structure.

Finally, it is common to find rhyodacite dykes on the margins of Cracow's mineralised structures (Fig. 1). The rhyodacite dykes generally dip subvertically and orientation analysis of their strikes indicates two populations exist in the Cracow area (Fig. 6). Some dykes intersected in drill core adjacent to the structures contain clasts of mineralised epithermal vein material, whereas others are cut by the structures, or have experienced the same distinctive epithermal alteration found in the wall rocks surrounding the faults. Thus, mutually overprinting relationships exist between the dykes and faults.

2.2. Fault rocks, deformation mechanisms and kinematics

A *fault core* is the internal zone of a fault (Fig. 2) comprising semi-continuous fault rock types that accommodated the majority of slip. Faults in sedimentary rocks tend to develop narrow fault cores (millimetres to metres) comprising slip surfaces and comminuted material (gouge, cataclasite and ultracataclasite), plus a surrounding *damage zone* of distributed fracturing and faulting (e.g. Chester and Logan, 1986; Schulz and Evans, 1998; Shipton and Cowie, 2001; Kim et al., 2004). Fault cores can be *paired* into two parallel but closely spaced cores, that link at depth or along-strike, and form a zone with a central domain of weakly deformed host rock (Childs et al., 1996). Some *paired fault cores* may arise from bifurcation of fault tip lines (Walsh et al., 2003) or because irregularities in the fault surface are shortcut (Watterson et al., 1998).

Fault-vein rock types in epithermal environments tend to comprise wide, cemented zones, with spectacular matrix-supported breccias and unique textures arising from the phase separation of water-rich fluids and CO_2 (White and Hedenquist, 1995). Cracow's epithermal structures are characterised by a main zone of fault rock, which is also the lode where the majority of gold is located. Progressive mining of single underground drives provided the opportunity to examine the mesoscopic fabrics and kinematics of Cracow's epithermal fault-vein rock types and their wall rock vein networks, plus the spatial variation of these attributes along strike. In the section below, I describe fault rock types and evaluate whether it is appropriate to apply the fault core-damage zone model to Cracow's epithermal fault-vein network. Then the wall rock vein networks and kinematics of the system are described.

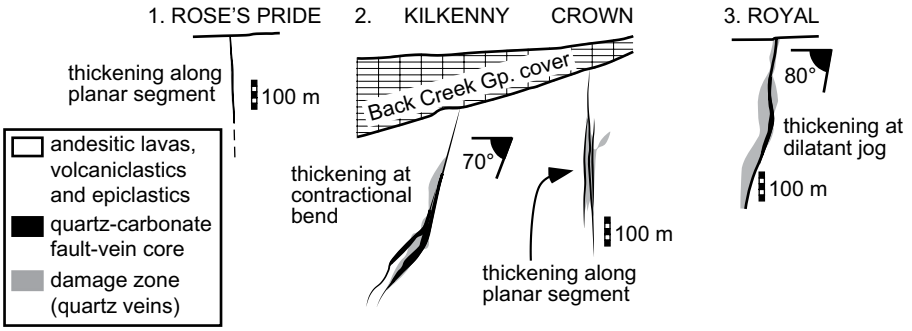

Fig. 4. Geometry of Cracow's faults in cross-section, sub-perpendicular to strike. Damage zones and fault-vein cores increase in thickness along planar fault patches, at contractional bends and dilatant jogs. See Fig. 1 for the location of each cross-section.

2.2.1. Fault rocks

Fault-vein rocks associated with epithermal mineralisation at Cracow form remarkably thick zones (4–10 m) of matrix supported breccias, laminated cements and cataclasites, and they consistently dip steeply west at 70–90° (Figs. 4 and 5). Four different fault rock types were identified on the basis of mesoscopic fabrics (Fig. 7). (1) Massive breccias and laminated zones, cemented by quartz–carbonate+/−adularia (qz-carb+/−adul), which are continuous along-strike (hundreds to thousands of metres). Typically cement-supported, these breccias have clast sizes ranging from metre-long blocks to clasts on the centimetre scale. Clasts are composed of both host-rock fragments or pre-existing lode, indicating this rock type formed from multiple events that re-brecciated the lode. Laminated zones tend to have planar margins. (2) Jigsaw breccias, comprising host-rock clasts that match together but are separated by mm–cm layers of carbonate and quartz. The jigsaw texture indicates low-strain, dilatant fracturing with negligible shear component. These breccias form semi-continuous domains along-strike, often on the margins of central zones of fault rock, or in association with wall rock between two closely spaced zones (Figs. 7 and 8). (3) Poorly sorted cataclasites, or breccias with fragments of wall-rock and rock-type 1, plus a matrix of rock flour. They tend to be discontinuous along-strike (tens of metres). Drive C1964 in Fig. 7a shows this cataclasite occupying fractures in rock-type 1. Large fragments of qz-carb material from rock-type 1 are also assimilated into the cataclasite, with some breccia textures suggesting grading. (4) Discrete, clay-rich, cataclastic fault planes are localised along or adjacent to the main zone of fault rock, and occasionally crosscut that zone (Fig. 8a). Most of the clay-rich faults contain small, spaced fragments of lode or wall-rock (<1 mm diameter) and are jacketed by margins of clay alteration. They are semi-continuous in length but nearly always present, crosscutting all vein material that they intersect, suggesting they have a late timing relative to the lodes.

Systematic crosscutting relationships exist between the different fault rock types in different places. For example, in drive C1964 (Fig. 7a) the hangingwall margin of fault rock layer 1 is crosscut by layer 2. In turn layer 2 is fragmented and incorporated into the cataclasite of layer 3. Similar crosscutting sequences were observed in a number of different drive faces. Each textural increment is localised on the hangingwall margins of pre-existing fault rock and the fault core appears to widen into the hangingwall.

Cracow's epithermal structures are dominated by thick zones of fault rock containing the fault rock types described above. Host lithology can change across these zones and as already demonstrated,

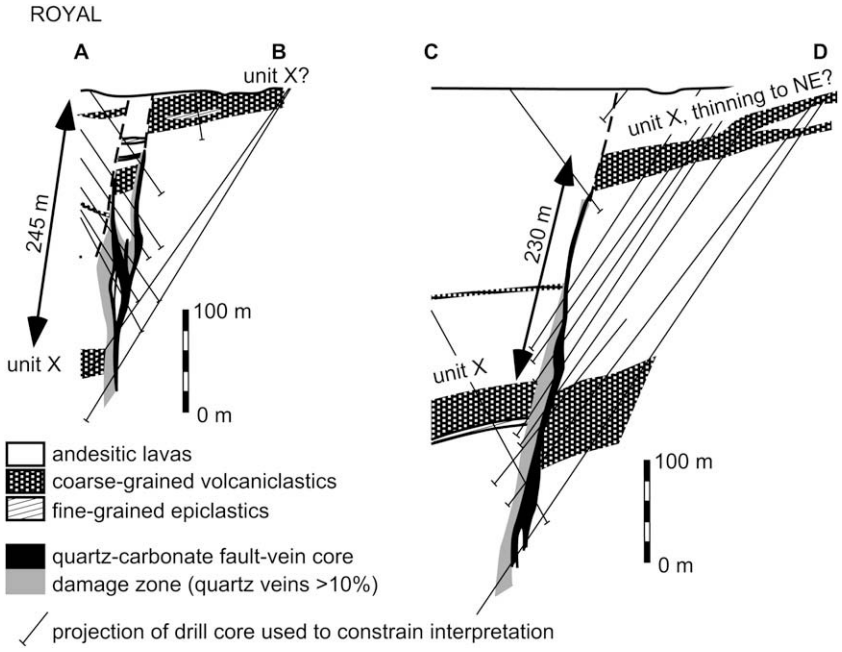

Fig. 5. Cross-sections of the Royal lode and stratigraphic marker units providing offset information. The thickness of fault-vein cores and damage zones varies down dip and normal offsets of stratigraphy are ~250 m. See Fig. 1 for the location of cross-section A–B and C–D.

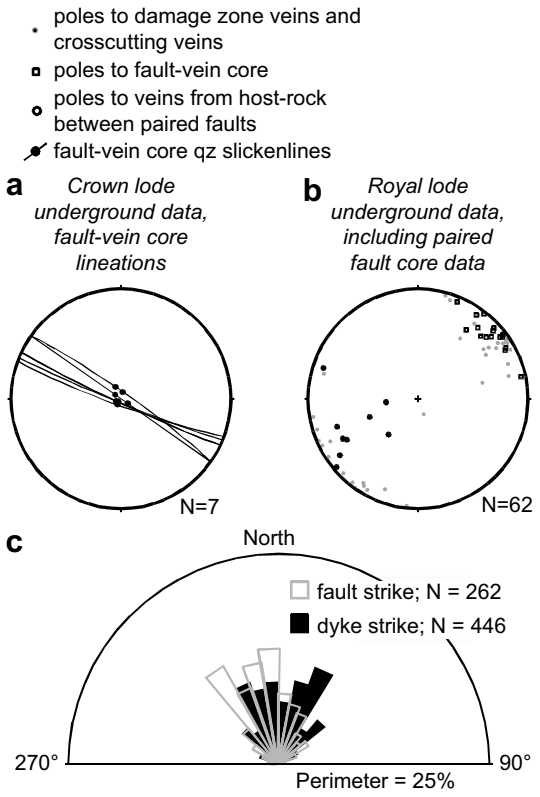

Fig. 6. Kinematic data from the Crown lode, Royal lode, and comparisons of dyke versus fault orientations. (a) At the Crown lode, rare slickenlines are pure dip-slip. (b) At the Royal lode, poles to veins, measured from the host rock within a paired fault core, show a trend from steep to subhorizontal orientations indicating rotation. (c) The rose diagram shows two populations of coactive dykes can be distinguished on the basis of their strike. One of these populations is consistent with normal dip-slip on the majority of fault planes, whereas the other suggests oblique-slip increments could have occurred on the NW–SE oriented fault system.

up to 300 m of displacement accumulated, even though the textures of the fault rocks indicate large components of dilatancy. The fault rock zone can be up to 10 m thick, but it is also associated with surrounding extension veins and shear veins with small-displacements, which are at most 30 cm thick and distributed over tens of metres into undeformed wall rock. Thus there seems to be a central fault core accommodating the majority of displacement, with a surrounding domain of cemented fractures and shear features. The density of wall rock veins does not increase towards the fault core, except in rare places. For these reasons the fault core-damage zone model appears to be appropriate for Cracow's epithermal fault-vein system; rather than a model where the main fault rock zone forms from an increasing density and amalgamation of distributed small-displacement veins and breccias.

Finally, parallel but closely spaced zones of fault rock (i.e. paired fault cores) are irregularly developed from single fault-rock zones, both along strike and down dip (Fig. 8), separated by a central zone of deformed and veined host-rock (1–3 m thick). Both single and paired fault cores are jacketed by relatively small amounts of visible cream-yellow alteration of their immediate wall-rock (illitic–smectitic clays). The width of visible wall rock alteration is highly variable along strike (0.01 m up to 0.5 m).

2.2.2. Damage zones

Fault damage zones are dominated by networks of extension and shear veins (traditionally termed "stockwork"). A critical observation is that damage zone veins have a large range of orientations (Fig. 9), which contrasts with the restricted orientations of the fault cores that they surround. Vein orientation data collected from underground exposures of the Crown lode revealed a northwest striking, steeply dipping fault-vein core. However, adjacent damage zone extension veins have a large range of strike and dip orientations, which describe a broad girdle (Fig. 9). Furthermore, the different vein orientations in the damage zones have mutual crosscutting relationships. A good example of this is shown in Fig. 8c, where two steeply dipping veins are oriented perpendicular to one another. A banded vein bisects a milky quartz vein but half of the width of the banded vein is also crosscut by the quartz vein, though its median line is not disrupted. Elsewhere, the milky quartz vein crosscuts and offsets a splay of the banded vein. Recent models of fracture growth have demonstrated that fractures with oblique or even perpendicular orientations to each other can, in some circumstances, open and propagate simultaneously (Healy et al., 2006; Blenkinsop, 2008) under a single far-field stress. In this example (Fig. 8c), the different mineralogies and mineral textures in the intersecting veins cannot be explained by synchronous opening, but a cyclical deformation history (Potts and Reddy, 1999), where each vein opened at different times and crosscut the other. The wide range of vein orientations and mutual crosscutting relationships are better explained by transient changes in the orientations of the principal stresses, at least locally, during successive vein opening increments.

In addition to orientation, the density of damage zone veins is highly variable along-strike (over tens of metres) and between footwall and hangingwall. In some places the wall rock veins are not present at all, even when the fault core is well-developed. In other places they are developed only in the hangingwall, or only in the footwall. Some rare veins crosscut parts of the fault core, although mostly the fault core crosscuts damage zone veins (e.g. Fig. 7), suggesting damage zone veins formed throughout the active lifetime of the fault cores rather than just arising during the early stages of fault development. The wall rock veins are associated both with remarkably planar fault core margins and more rarely with chaotic margins, where the damage zone merges into the main fault core with vein networks of increasing density.

Drive C2000 (Fig. 7d) exposed a fault core containing metre-scale, wall rock fragments, which are associated with a planar lode margin and subvertical, vein networks in a footwall damage zone. The footwall veins become asymptotic with and linked into the fault-vein core, creating large rhombic fragments of wall rock that match the geometry of the large clasts found within the fault-vein core. These observations suggest that in some circumstances wall rock fragments generated by damage zone veining were progressively incorporated into fault cores (Fig. 10), and contributed to the development of fault rock, via deformation mechanisms of wall rock fracture, veining, intra- and interclast fragmentation, and finally assimilation.

2.2.3. Kinematics

Evidence for the movement direction of Cracow's epithermal faults arises from a number of independent observations. On the fault system scale, stratigraphy has a normal offset across mineralised structures (Fig. 5), and the apparent separation vectors (Nortje et al., 2006) of breccia textures exposed in drive faces indicate that a normal extensional-shear mode of failure operated in the fault-vein cores. Drive faces from C2000 and C1982 (Fig. 7) contain metre-scale wall rock clasts with apparent separation vectors indicating normal slip and opening. However, significant oblique-slip could have still occurred out of the plane of view (Nortje et al., 2006).

Direct evidence that the measured normal offsets of stratigraphy arise from dip-slip movement comes from rare qz-carb slickenlines, measured from underground exposure of the margins

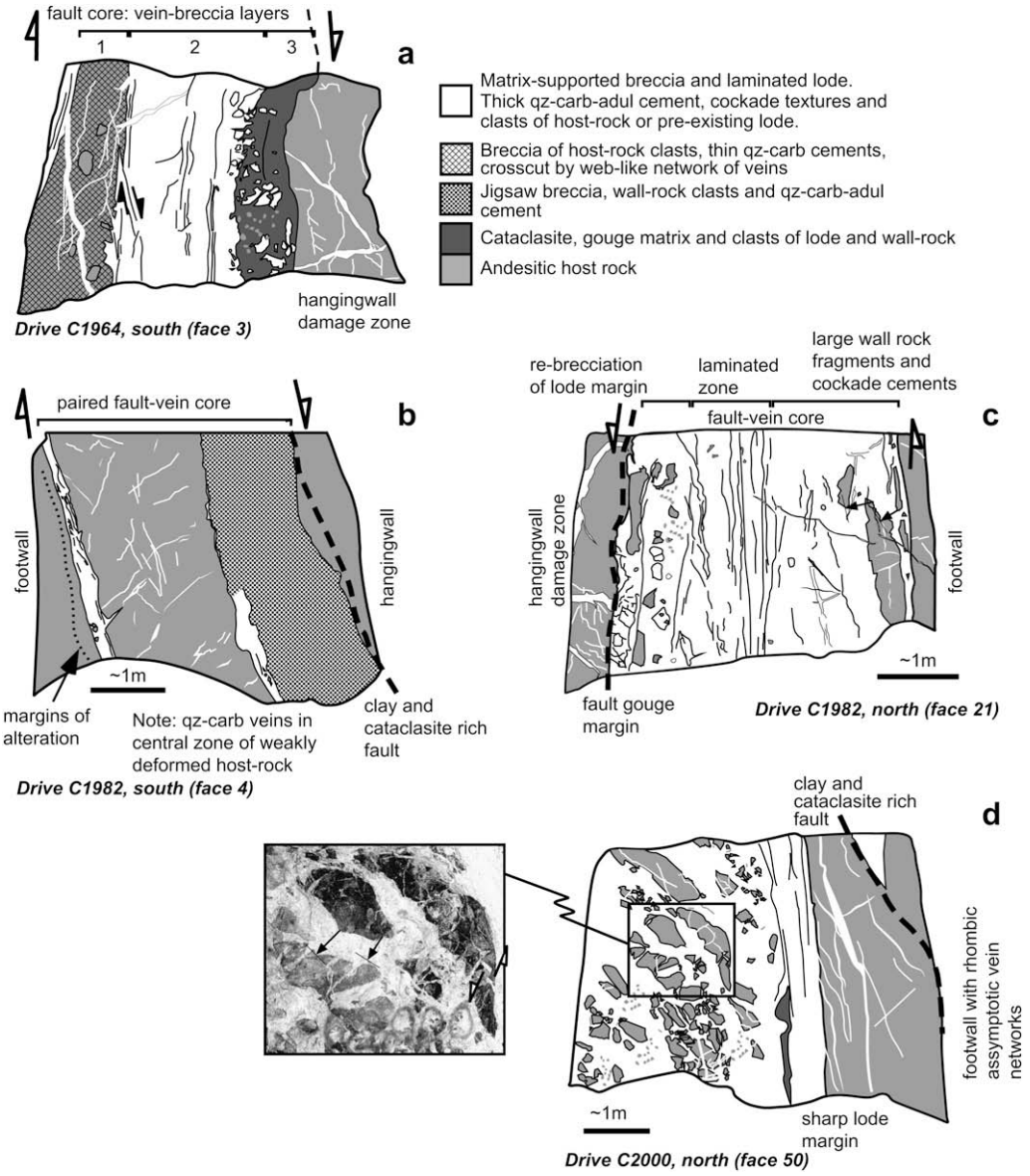

Fig. 7. Sketches of fault rock textures from Cracow's qz-carb, epithermal fault-vein cores, at different drive faces of the Crown lode. A variety of fault rock textures exist in each drive face. Relative to the lodes, damage zone veins have a range of apparent orientations. The density of damage zone veins varies from face to face. Breccia textures at (c) drive C1982, north face and (d) C2000, north face preserve apparent normal dip-slip-opening vectors.

of the Crown lode (Fig. 6). Further kinematic evidence comes from the orientations of veins measured from deformed pods of host-rock in paired fault cores, from the Royal lode. Measured orientations indicate that the veins within the host-rock pod have been rotated between the slip surfaces either side of it, consistent with a normal movement (Fig. 6). Thus, overall the kinematics of Cracow's epithermal faults can be described by normal-slip movement, with a component of opening.

However, small displacement features (>1 m), show more variable kinematics, and this variation has no obvious relationship with fault geometry or location. A shear vein preserved in the Royal lode's R1909 stope had stepped quartz slickenfibres, indicating dextral reverse movement (Fig. 8b). Small, cataclastic, clay-rich faults in both the Crown and Royal lodes preserve lineations and offsets that indicate normal, oblique and strike-slip movements, sometimes in the same drive face. Also, as already noted, vein orientations from the wall rocks occupy a wide range of orientations (Fig. 9).

Further evidence, for at least transient variations in the kinematics of the system comes from an analysis of mapped orientations of dykes across the region, interpreted to be coeval with epithermal mineralisation. In volcano-tectonic terrains dykes can be used to indicate the orientation of a regions stress field at the time of intrusion, assuming dykes open parallel with the maximum principal stress according to the tensile failure criterion. At Cracow, two populations of steeply dipping rhyodacite dykes can be defined on the basis of their strike orientations (Fig. 6). One of these populations is consistent with normal slip on the mineralised fault system. However, a second population of dykes with a northeast strike, are consistent with oblique to dextral strike-slip movement on the mineralised faults.

3. Review and interpretation

This section reviews existing models on the formation of epithermal deposits, interprets the kinematic and permeability

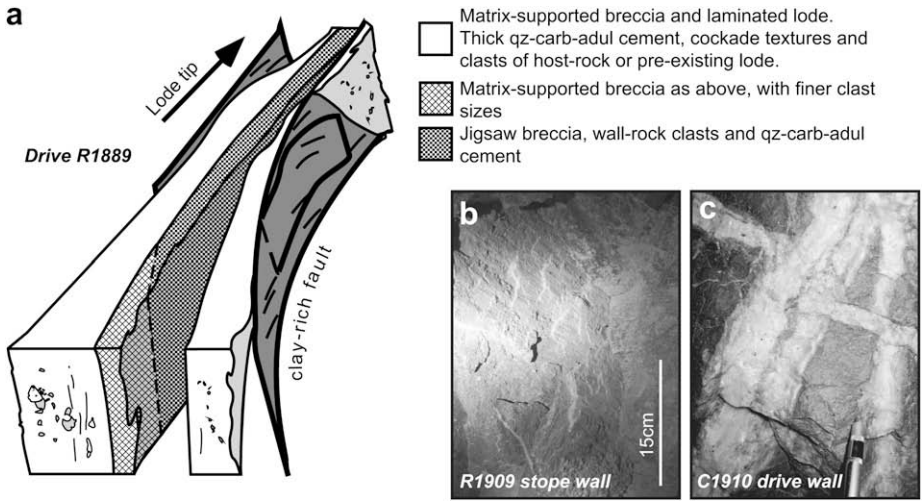

Fig. 8. (a) 3-D construction of the Royal lode, taken from photos and sketches during progressive mining of the drive face R1889. (b) Quartz slickenfibres showing dextral-reverse movement occurred during mineral growth, from a shear vein in the Royal lode damage zone. In cross-section the vein exhibits banded, epithermal crustiform vein textures. (c) Perpendicular but mutually crosscutting veins from a damage zone in the Crown lode.

enhancement processes operating in epithermal systems like the Cracow goldfield, and compares that interpretation with observations of fault behaviour in active geothermal environments.

In order for economic-grade deposits to form, focused fluid flow and efficient metal deposition mechanisms are critical (Simmons and Browne, 2000; Simmons and Brown, 2006). A number of models of fault-vein hosted epithermal deposits have been proposed (e.g. White, 1955; Buchanan, 1981; Henley, 1985; White and Hedenquist, 1995). Notably, the models share common characteristics such as a hydrological regime dominated by fluid convection, hydrostatic fluid pressures, gold mineralisation due to phase separation ("boiling") of largely meteoric waters and formation of deposits at depths less than 1.0 km. Convecting meteoric fluids are envisaged to ascend open fault-fracture networks, and undergo phase separation of CO_2 and H_2S, which destabilises gold in solution. The shared characteristics of the models are in part due to the models being strongly informed by mineralogical, thermal and geochemical observations of geothermal fields with convecting hydrothermal fluids, which are exploited for their energy (White, 1981; Clark and Williams-Jones, 1990; Simmons and Browne, 2000; Simmons et al., 2006).

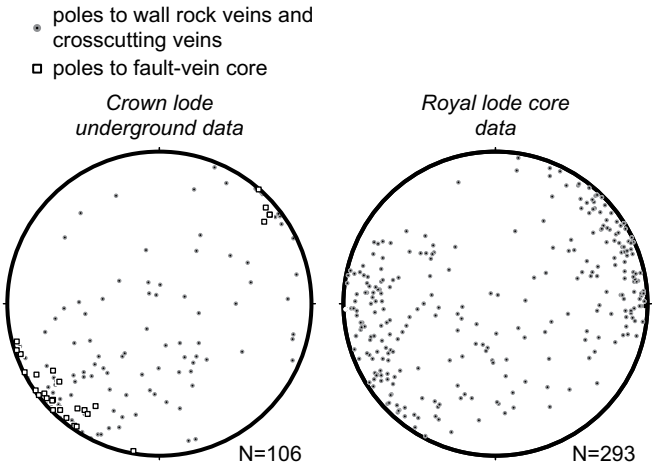

Fig. 9. Orientations of poles to both fault-vein cores and wall rock veins from the Crown lode, and wall rock veins from the Royal lode.

However, an intriguing relationship exists between the distribution of fault systems and convecting geothermal fluid cells in the Taupo Volcanic Zone (Rowland and Sibson, 2004). Geothermal fields are mostly located around the margins of dense fault networks (Fig. 11). Close inspection shows that faults can act as effective aquitards, although upflow zones do develop at fault tips and stepovers (Rowland and Sibson, 2004). Even in rock units with high host rock matrix permeability, fault-related fluids deposit silica phases, cement local porosity and dramatically alter the local strength and permeability properties of the host rock (Hancock et al., 1999; Rowland and Sibson, 2004). Fault-related permeability enhancement can be highly episodic (e.g. Sibson, 1987; Tenthorey et al., 2003; Micklethwaite and Cox, 2004; Cox, 2005; Davatzes and Hickman, 2005; Woodcock et al., 2007), and an implication is that epithermal mineralisation may be forming in fault networks which are only transiently permeable, away from actively convecting fluid cells.

3.1. Failure mode and fluid pressure variations

The relationship between stress magnitude, fluid pressure, failure mode and fault dip during fault formation can be derived (Fig. 12), using a composite Griffith-Coulomb failure criterion and appropriate friction values (Secor, 1965; Walsh and Watterson, 1988; Micklethwaite, 2008). At Cracow, host rock composition is

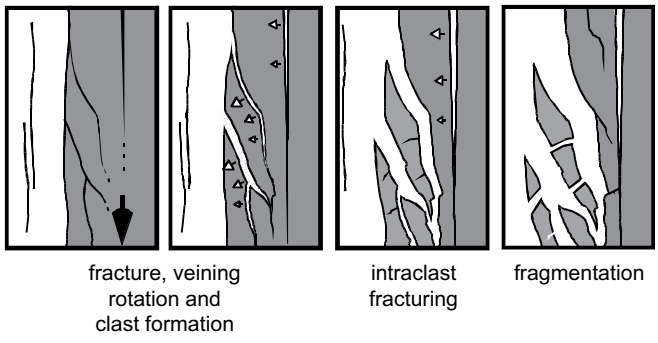

Fig. 10. Interpretation of the development of cement supported breccias, with metre-sized clasts and extensional-shear textures (e.g. see example in Fig. 6d). From left to right, wall rock fractures propagate, veins develop and chunks of wall rock fragment into the fault vein core.

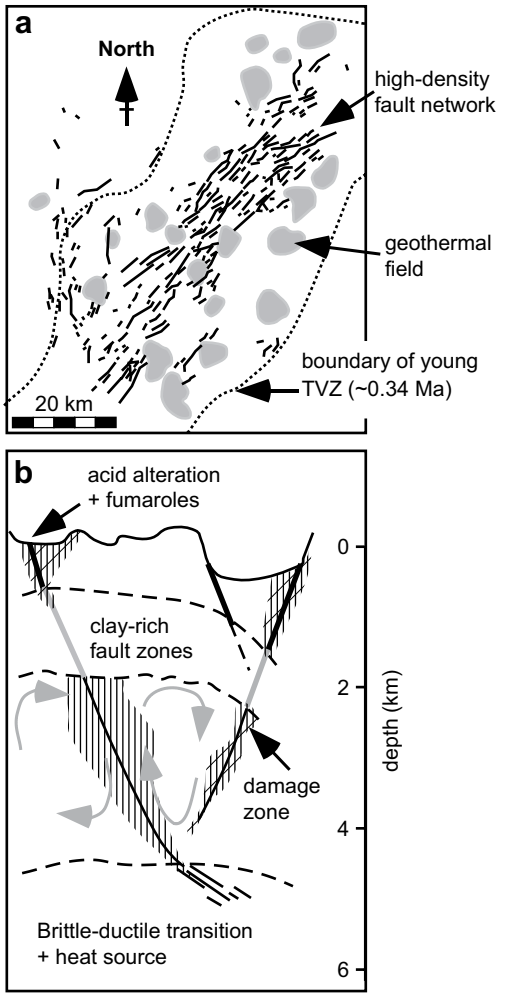

Fig. 11. (a) Map of the Taupo Volcanic Zone modified from Rowland and Sibson (2004). Geothermal fields are distributed around the margins of dense fault networks. (b) Cross-section illustrating the relationships observed in the Coso geothermal field, modified from Davatzes and Hickman (2005). Clay alteration on normal faults, seals the faults and prevents escape of convecting, overpressured fluids trapped at >2 km depth.

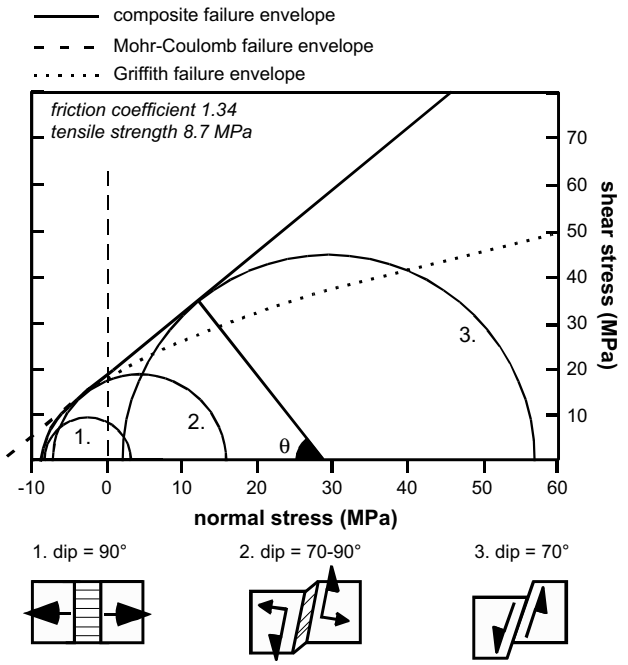

Fig. 12. Mohr diagram showing the dip orientations and failure mode of fractures developed in andesitic lava. Failure mode and fracture dip is a function of differential stress magnitude, illustrated by three different Mohr stress circles. Fluid pressure lowers mean stress and drives stress circles to the left in the diagram. Fracture dip is calculated from the normal to the failure envelope at the point where stress circles contact the failure envelope. At low differential stresses, stress state 1 leads to tensile failure and subvertical fractures. At slightly larger differential stresses, stress state 2 leads to shear-opening failure with fracture dips of 70–90°, whilst at moderate to large differential stresses fractures fail by shear failure alone with dips of 70°. Assuming an Andersonian stress regime with vertical maximum principal stress and subhorizontal minimum principal stress perpendicular to the strike of fractures then vertical stress is related to lithostatic pressure minus fluid pressure, and can therefore be related to depth (e.g. Walsh and Watterson, 1988).

dominated by andesitic lavas. The internal coefficient of friction for andesites can have unusually high values (1.2–1.9; Ozsan and Akin, 2002; Moon et al., 2005). In normal fault environments, where the maximum principal stress is the overburden pressure, the composite failure criterion predicts that faulting, by frictional shear failure of andesite, occurs at dips of 70° (Fig. 12). Mixed mode extensional-shear will develop dips between 70–90° and pure extension veins are expected to be subvertical. Fault dip data from Cracow agree with the calculated theoretical values (Fig. 13), ranging between 70° and 90°, with minimum dip values clustering towards 70°. The data indicate extensional-shear and pure extension were important failure mechanisms at Cracow. Field observations support this conclusion with multiple, extensional-shear events indicated by both the textures of some cement-supported breccias, as well as normal displacements of up to 250 m across wide, cement-supported fault cores.

Because epithermal deposits are thought to form at shallow crustal levels (<1.0 km) in extensional regimes, pure extension or extensional-shear failure do not necessarily require elevated fluid pressures to occur. This is unusual compared to vein formation in other types of mineral deposit where fluid overpressures are necessary for vein formation (e.g. Micklethwaite, 2008). Nevertheless, underground drive face exposures at Cracow revealed a range of different fault rock textures are preserved at each point on the faults. These include jigsaw breccias requiring pure extension, cement-supported breccias suggesting extensional-shear, and cataclasites or gouge arising from shear failure. This variety of fault rock types at a single location on a fault surface could arise from fluctuations in fluid pressure and differential stress (Fig. 12).

Elevated fluid pressures are important for fault failure in active geothermal environments, because spectacular swarms of earthquakes can be triggered even by small stress changes induced by the passage of seismic waves from distant large earthquakes (Hill et al., 1993, 1995; Gomberg et al., 2001; Husen et al., 2004; Brodsky and Prejean, 2005), suggesting faults are sometimes close to failure. Likewise, non-double-couple earthquake focal mechanisms observed in geothermal environments are consistent with faults failing under elevated pore fluid pressures, with a mixed mode of extensional-shear failure, accompanied by the rapid flow of aqueous or CO_2-rich fluids into open fractures (Dreger et al., 2000; Foulger et al., 2004; Templeton and Dreger, 2006).

3.2. Transient kinematic variation

The kinematics of faults associated with many epithermal deposits are elusive and difficult to determine (e.g. Nortje et al., 2006), and when slip directions have been determined faults display a range of slip directions, including strike-slip and dip-slip movement (Brathwaite and McKay, 1983; Berger et al., 2003). Here, Cracow's epithermal faults exhibit predominantly normal dip-slip kinematics, but strike-slip and oblique-slip kinematics (including

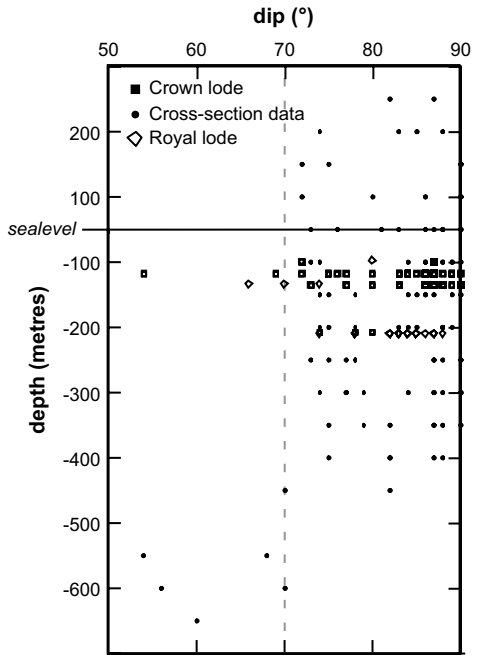

Fig. 13. Fault dip data of Cracow's dilatant, epithermal fault-vein cores, relative to depth. Dip data falls in the range 70–90°.

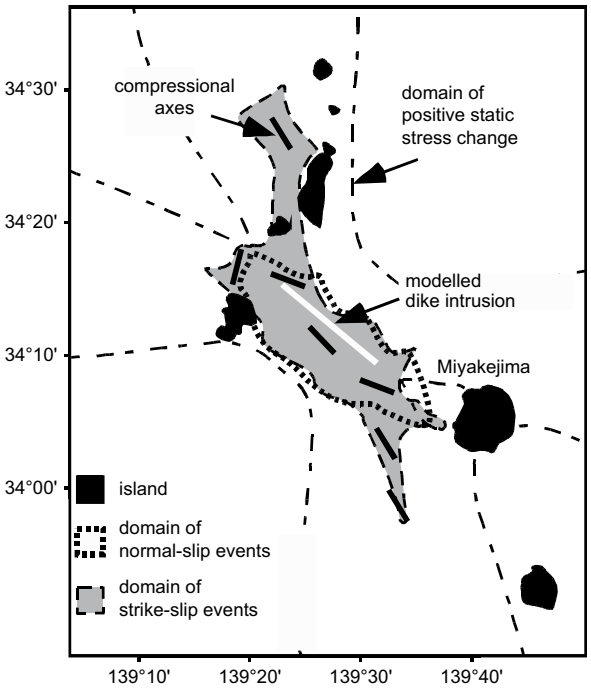

Fig. 14. Dyke, fault and stress relationships observed during the 2000 Miyakejima volcanic eruption and dyke intrusion, compiled from Fukuyama et al. (2001), and Toda et al. (2002). Faults hosted normal-slip earthquakes in the flanks of the dyke, and strike-slip earthquakes in a dog-bone pattern around the dyke. The orientations of compressional axes, determined from earthquake focal mechanisms, rotate relative to the location of the dyke. Seismicity also correlates with the distribution of static stress changes calculated for the intrusion and inflation of the dyke.

reverse components) are also preserved. Another critical observation is that wall-rock veins, associated with Cracow's faults, have a large range of orientations. Finally, veins of different orientations have mutual crosscutting relationships.

In this study, the range of fault kinematics and of damage zone vein orientations are interpreted to relate to the dynamics of the geothermal environment where Cracow formed—namely the intrusion and inflation of adjacent dykes transiently changing the local stress state and inducing fluctuations in fault kinematics. Both the Crown and Royal lode are spatially and temporally associated with dykes, and dykes have intruded across the Cracow area. Coeval magmatic activity, such as the intrusion of dykes, has a significant influence on the location, kinematics and triggering of fault slip-events (Fig. 14; Hill, 1977; Fukuyama et al., 2001; Toda et al., 2002; Gudmundsson et al., 2008). Static stress change models show the propagation and inflation of intruding dykes can disrupt the orientations of regional stresses in the near-field to dykes (Roman and Heron, 2007) and lead to transient variations in fault kinematics. This process has been observed in Yellowstone National Park, USA and off the SE coast of Japan. Waite and Smith (2002) documented the October 1985, Yellowstone earthquake swarm, where the kinematics of earthquakes on normal-dip slip faults switched and generated oblique and strike-slip earthquakes, indicating a large local rotation of stress orientations, due to intrusion of a dyke. Dyke intrusion during the 2000 Miyakejima eruption triggered the largest earthquake swarm on historical record (Fukuyama et al., 2001). Stress changes during inflation of the dyke (Fig. 14) resulted in thousands of normal fault earthquakes on its flanks, but strike-slip earthquakes both on its flanks and in a dog-bone pattern off the tips of the dyke (Fukuyama et al., 2001; Toda et al., 2002). These studies demonstrate that depending on the location of an intruding dyke, a normal slipping fault can transiently develop oblique, strike-slip, or even reverse kinematics (e.g. Gudmundsson et al., 2008).

3.3. Permeability enhancement processes

The above considerations suggest the existence of three first-order processes controlling permeability during epithermal faulting at Cracow. (1) Kinematic change on a corrugated fault surface (Fig. 15a): Because Cracow's faults are corrugated along strike reflecting normal-slip movement (i.e. corrugation axes down the dip of the fault), any oblique-slip increment has the potential to temporarily enhance permeability parallel with the dip of the fault plane. This transient mechanism may explain the existence of subvertical shoots of precious-metal mineralisation along some planar epithermal fault segments. (2) Fault-related geometry: Many normal fault systems develop jogs and bends down the dip of the fault plane. Where fault orientation steepens, subhorizontal extension leads to veining and fracturing, and enhancement of permeability approximately parallel with the strike of the fault plane. However, fault curvature is also an important aspect of faults in volcano-tectonic environments, with faults steepening and fissuring towards the Earth's surface (e.g. Grant and Kattenhorn, 2004). This may explain the subvertical dip of some of Cracow's faults (Fig. 13). Any slip events on faults exhibiting such curvature would induce extension or extensional-shear failure near the surface, and enhance permeability along the full strike length of a fault segment. (3) Fluid pressure driven opening (Fig. 15b): In addition to mechanism 2, fault surfaces can fail by extensional-shear when near-surface fault curvature is not a factor. Increases in fluid pressure, or migrating pulses of overpressured fluids, plus low differential stresses, can induce extensional-shear failure of fault surfaces at depth. Fluid pressure drops associated with rupture of a fault plane can lead to phase separation and "boiling" of hydrothermal fluids at greater depths than predicted by hydrostatic fluid pressure models (Sibson, 1987). The latter process may operate in the Coso geothermal field, USA (Davatzes and Hickman, 2005), where qz-carb breccias and vein material are found at depths >2 km, associated with a compartment of convecting overpressured fluids (Fig. 11). In Cracow's fault system, fluid pressure

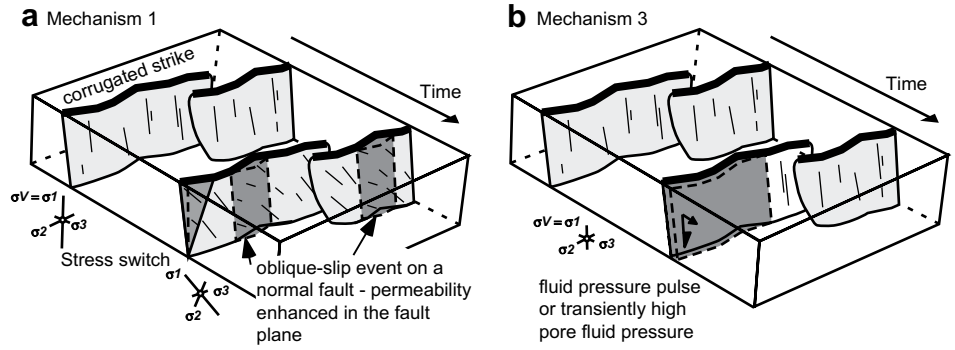

Fig. 15. Permeability enhancement mechanisms 1 and 3. (a) Switches in incremental fault slip kinematics, driven by transient changes in stress orientation, leads to dilation parallel with the dip of faults which have corrugated strikes. (b) Migration of pulses of overpressured fluid or overpressured pore fluids, under low differential stress, enables extensional-shear/extensional failure and permeability enhancement in the plane of the fault.

driven failure feasibly explains the observation of thickening of qz-carb fault-vein cores at unusual locations, such as contractional bends. Again this mechanism will enhance permeability along the strike length of a fault segment and not just at the fault tips or step-over zones of a system.

Previous epithermal models of precious metal mineralisation in geothermal environments do not consider the geodynamic behaviour of these environments. Fluid pressure and stress states are not static, which must be accounted for in physical and chemical models. The scale of the fluid plumbing system in epithermal environments is on the order of 5–6 km deep, and faults may only need to breach to depths of 1–3 km in order to tap overpressured fluid reservoirs, magmatic fluids or deeply circulating meteoric waters. As a result, quite small fault systems (1–3 km long) are sufficient to generate the conditions necessary for mineralisation. Significantly, the majority of fault-related permeability enhancement is temporally transient, suggesting that fault-vein hosted epithermal mineralisation is a not a steady-state process.

4. Conclusions

Epithermal fault-vein networks at Cracow developed a distinct central fault core with normal offsets up to 300 m, comprising multiple increments of breccias, surrounded by a damage zone of extensional and shear veins. Damage zone veins vary in distribution, orientation and density. Epithermal fault-vein systems differ from other types of fault systems in that the fault cores can be extremely thick (up to 10 m), due to large components of dilation and quartz cementation during failure.

Cracow's fault-vein network was dominated by normal dip-slip movement, but slip directions and vein orientations transiently varied to reflect strike-slip and even oblique-reverse slip movement. This kinematic complexity is not related to fault geometry or location but is attributed to transient stress rotation because of coeval intrusion of adjacent dykes. Similar processes have been observed in active geothermal environments.

Transient variations in slip direction of Cracow's faults would have enhanced permeability along the fault plane, parallel with fault plane corrugations; potentially leading to the development of ore shoots approximately parallel with the dominant slip direction. Permeability enhancement was also controlled by well-documented processes such as fluid pressure driven failure and the steepening of faults near-surface or at down-dip jogs. This variety of mechanisms may explain the large variations of gold grade and gold distribution observed in epithermal systems.

Effective fluid focusing occurred along planar fault segments, as well as at step-overs or fault tip zones. The ruptured fault surfaces likely sealed rapidly, although a small percentage of fractures may have remain open for extended periods of time. Accordingly epithermal mineralisation is not a steady-state process but is dependent on pulses of fluid flow associated with transient permeability enhancement processes.

Acknowledgements

This research was supported by Barrick Gold, Gold Fields, Newcrest and Newmont (through AMIRA International) and an associated Australian Research Council Linkage grant. Generous help and logistical support was provided at Cracow by Simon Shakesby, Chris Chambers, Trinity Gilmore, Ben Spence, Rob Taube, Corrie Chamberlain and James Francis. Newcrest provided geological, geophysical and drill-core data for the map and cross-section interpretations presented in this paper, but any errors in interpretation are my own. The study benefited from discussions with Zoe Shipton and Rebecca Lunn, made possible by a Royal Society of Edinburgh International Exchange travel grant. Reviews by John Walsh and Julie Rowland, the editorial assistance of Bob Holdsworth and an informal review by Stephen Cox greatly improved the manuscript.

References

Allen, C.M., 2000. Evolution of a post-batholith dike swarm in central coastal Queensland, Australia: arc-front to backarc? Lithos 51, 331–349.

Allen, C.M., Williams, I.S., Stephens, C.J., Fielding, C.R., 1998. Granite genesis and basin formation in and extensional setting: the magmatic history of the northernmost New England Orogen. Australian Journal of Earth Sciences 45, 875–888.

Bailey, W.R., Walsh, J.J., Manzocchi, T., 2005. Fault populations, strain distribution and basement fault reactivation in the East Pennines Coalfield, UK. Journal of Structural Geology 27, 913–928, doi:10.1016/j.jsg.2004.10.014.

Barton, C.A., Zoback, M.D., Moos, D., 1995. Fluid flow along potentially active faults in crystalline rock. Geology 23, 683–686.

Berger, B.R., Tingley, J.V., Drew, L.J., 2003. Structural localization and origin of compartmentalized fluid flow, Comstock Lode, Virginia City, Nevada. Economic Geology 98, 387–408.

Blenkinsop, T.G., 2008. Relationships between faults, extension fractures and veins, and stress. Journal of Structural Geology 30, 622–632.

Brantley, S.L., 1992. The effect of fluid chemistry on quartz microcrack lifetimes. Earth and Planetary Science Letters 113, 145–156.

Brathwaite, R.L., McKay, D.F., 1983. Geology and exploration of the Martha Hill gold-silver deposit, Waihi. Australasian Institute of Mining and Metallurgy, Monograph 13, 83–88.

Braund, K., 2006. Geology, geochemistry and paragenesis of the Royal, Crown and Roses Pride low sulphidation epithermal quartz vein structures, Cracow, South-East Queensland. Masters Thesis, University of Queensland.

Brodsky, E.E., Prejean, S.G., 2005. New constraints on mechanisms of remotely triggered seismicity at Long Valley Caldera. Journal of Geophysical Research 110, B04302, doi:10.1029/2004JB003211.

Buchanan, L.J., 1981. Precious metal deposits associated with volcanic environments in the southwest. Arizona Geological Society Digest 14, 237–262.

Bull, J.M., Minshull, T.A., Mitchell, N.C., Dix, J.K., Hardardottir, J., 2005. Magmatic and tectonic history of Iceland's western rift zone at Lake Thingvallavatn. Geological Society of America Bulletin 117, 1451–1465.
Bull, J.M., Barnes, P.M., Lamarche, G., Sanderson, D.J., Cowie, P.A., Taylor, S.K., Dix, J.K., 2006. High-resolution record of displacement accumulation on an active normal fault: implications for models of slip accumulation during repeated earthquakes. Journal of Structural Geology 28, 1146–1166.
Caine, J.S., Evans, J.P., Forster, C.B., 1996. Fault zone architecture and permeability structure. Geology 24, 1025–1028.
Chester, F.M., Logan, J.M., 1986. Implications for mechanical properties of brittle fault from observations of the Punchbowl Fault Zone, California. Pure Applied Geophysics 124, 79–106.
Childs, C., Watterson, J., Walsh, J.J., 1996. A model for the structure and development of fault zones. Journal of the Geological Society of London 153, 337–340.
Clark, J.R., Williams-Jones, A.E., 1990. Analogues of epithermal gold-silver deposition in geothermal well scales. Nature 346, 644–645.
Cowie, P.A., 1998. A healing-reloading feedback control on the growth rate of seismogenic faults. Journal of Structural Geology 20, 1075–1087.
Cowie, P.A., Scholz, C.H., 1992. Displacement-length scaling relationships for faults: data synthesis and discussion. Journal of Structural Geology 14, 1149–1156.
Cox, S.F., 2005. Coupling between deformation, fluid pressures and fluid flow in ore-producing hydrothermal systems at depth in the crust. Economic Geology 100th Anniversary Volume, 1–35.
Cox, S.F., Braun, J., Knackstedt, M.A., 2001. Principles of structural control on permeability and fluid flow in hydrothermal systems. Reviews in Economic Geology 14, 1–24.
Curewitz, D., Karson, J.A., 1997. Structural settings of hydrothermal outflow: Fracture permeability maintained by fault propagation and interaction. Journal of Volcanology and Geothermal Research 79, 149–168.
Dawers, N.H., Anders, M.H., Scholz, C.H., 1993. Growth of normal faults: Displacement-length scaling. Geology 21, 1107–1110.
Davatzes, N.C., Hickman, S.H., 2005. Controls on fault-hosted fluid flow; Preliminary results from the Coso geothermal field, CA. Geothermal Research Council Transactions, paper 144.
Dong, G.Y., Zhou, T., 1996. Zoning in the Carboniferous-Lower Permian Cracow epithermal vein system, central Queensland, Australia. Mineralium Deposita 31, 210–224.
Dreger, D.S., Tkalcic, H., Johnston, M., 2000. Dilational processes accompanying earthquakes in the Long Valley Caldera. Science 288, 122–125.
Evans, J.P., Forster, C.B., Goddard, J.V., 1997. Permeability of fault-related rocks, and implications for hydraulic structure of fault zones. Journal of Structural Geology 11, 1393–1404.
Fairley, J.P., Hinds, J.J., 2004. Field observation of fluid circulation patterns in a normal fault system. Geophysical Research Letters 31, L19502, doi:10.1029/2004GL020812.
Foulger, G.R., Julian, B.R., Hill, D.P., Pitt, A.M., Malin, P.E., Shalev, E., 2004. Non-double-couple microearthquakes at Long Valley caldera, California, provide evidence for hydraulic fracturing. Journal of Volcanology and Geothermal Research 132, 45–71.
Fukuyama, E., Kubo, A., Kawai, H., Nonomura, K., 2001. Seismic remote monitoring of stress field. Earth. Planets and Space 53, 1021–1026.
Gillespie, P.A., Walsh, J.J., Watterson, J., 1992. Limitations of dimension and displacement data from single faults and the consequences for data analysis and interpretation. Journal of Structural Geology 14, 1157–1172.
Gomberg, J., Reasenberg, P.A., Bodin, P., Harris, R.A., 2001. Earthquake triggering by seismic waves following the Landers and Hector Mine earthquake. Nature 411, 462–464.
Grant, J.V., Kattenhorn, S.A., 2004. Evolution of vertical faults at an extensional plate boundary, southwest Iceland. Journal of Structural Geology 26, 537–557.
Gudmundsson, A., Friese, N., Galindo, I., Philipp, S.L., 2008. Dike-induced reverse faulting in a graben. Geology 36, 123–126.
Hancock, P.L., Chalmers, R.M.L., Altunel, E., Çakir, Z., 1999. Travitonics: using travertines in active fault studies. Journal of Structural Geology 21, 903–916.
Healy, D., Jones, R.R., Holdsworth, R.E., 2006. New insights into the development of brittle shear fractures from a 3-D numerical model of microcrack interaction. Earth and Planetary Science Letters 249, 14–28.
Heffner, J., Fairley, J., 2006. Using surface characteristics to infer the permeability structure of an active fault zone. Sedimentary Geology 184, 255–265.
Henley, R.W., 1985. The geothermal framework for epithermal deposits. In: Berger, B.R., Bethke, P.M. (Eds.), Geology and Geochemistry of Epithermal Systems. Reviews in Economic Geology, 2, pp. 1–24.
Hill, D.P., 1977. A model for earthquake swarms. Journal of Geophysical Research 82, 1347–1352.
Hill, D.P., Reasenberg, P.A., Michael, A., Arabaz, W.J., Beroza, G., Brumbaugh, D., Brune, J.N., Castro, R., Davis, S., dePolo, D., Ellsworth, W.L., Gomberg, J., Harmsen, S., House, L., Jackson, S.M., Johnston, M.J.S., Jones, L., Keller, R., Malone, S., Munguia, L., Nava, S., Pechmann, J., Sanford, C.A., Simpson, R.W., Smith, R.B., Stark, M., Stickney, M., Vidal, A., Walter, S., Wong, V., Zollweg, J., 1993. Seismicity remotely triggered by the Magnitude 7.3 Landers, California, Earthquake. Science 260, 1617–1623.
Hill, D.P., Johnston, M.J.S., Langbein, J.O., 1995. Response of Long Valley caldera to the Mw=7.3 Landers, California, earthquake. Journal of Geophysical Research 100, 12985–13005.
Holcombe, R.J., Stephens, C.J., Fielding, C.R., Gust, D., Little, T.A., Sliwa, R., McPhie, J., Ewart, A., 1997. Tectonic evolution of the northern New England Fold Belt: Carboniferous to Early Permian transition from active accretion to extension. In: Geological Society, Australia, Special Publications, vol. 19, pp. 66–79.
Husen, S., Taylor, R., Smith, R.B., Healser, H., 2004. Changes in geyser eruption behavior and remotely triggered seismicity in Yellowstone National Park produced by the 2002 M 7.9 Denali fault earthquake, Alaska. Geology 32, 537–540.
Jones, J.A., Stephens, C.J., Ewart, A., 1996. Constraints on the Early Permian and Late Carboniferous of the Northern New England fold belt from the Camboon Volcanics and the Torsdale Beds: Geological Society of Australia. Abstracts 41, 222.
Kim, Y.-S., Peacock, D.C.P., Sanderson, D.J., 2004. Fault damage zones. Journal of Structural Geology 26, 503–517.
Micklethwaite, S., 2008. Optimally oriented "fault-valve" thrusts: Evidence for aftershock-related fluid pressure pulses? Geochemistry, Geophysics, Geosystems 9, Q04012, doi:10.1029/2007GC001916.
Micklethwaite, S., Cox, S.F., 2004. Fault-segment rupture, aftershock-zone fluid flow, and mineralization. Geology 32, 813–816.
Micklethwaite, S., Cox, S.F., 2006. Progressive fault triggering and fluid flow in aftershock domains: Examples from mineralized Archaean fault systems. Earth and Planetary Science Letters 250, 318–330.
Moon, V., Bradshaw, J., Smith, R., de Lange, W., 2005. Geotechnical characterisation of stratocone crater wall sequences, White Island Volcano, New Zealand. Engineering Geology 81, 146–178.
Muir-Wood, R., King, G.C.P., 1993. Hydrological signatures of earthquake strain. Journal of Geophysical Research 98, 22035–22068.
Nicol, A., Walsh, J., Berryman, K., Villamor, P., 2006. Interdependence of fault displacement rates and paleoearthquakes in an active rift. Geology 34, 865–868, doi:10.1130/G22335.1.
Nortje, G.S., Rowland, J.V., Sporli, K.B., Blenkinsop, T.G., Rabone, S.D.C., 2006. Vein deflections and thickness variations of epithermal quartz veins as indicators of fracture coalescence. Journal of Structural Geology 28, 1396–1405.
Ozsan, A., Akin, M., 2002. Engineering geological assessment of the proposed Urus Dam, Turkey. Engineering Geology 66, 271–281.
Peacock, D.C.P., Sanderson, D.J., 1991. Displacements, segment linkage and relay ramps in normal fault zones. Journal of Structural Geology 13, 721–733.
Potts, G.J., Reddy, S.M., 1999. Construction and systematic assessment of relative deformation histories. Journal of Structural Geology 21, 1245–1253.
Roman, D.C., Heron, P., 2007. Effect of regional tectonic setting on local fault response to episodes of volcanic activity. Geophysical Research Letters 34, L13310, doi:10.1029/2007GL030222.
Rowland, J.V., Sibson, R.H., 2001. Extensional fault kinematics within the Taupo Volcanic Zone, New Zealand: soft-linked segmentation of a continental rift system. New Zealand Journal of Geology and Geophysics 44, 271–283.
Rowland, J.V., Sibson, R.H., 2004. Structural controls on hydrothermal flow in a segmented rift system, Taupo Volcanic Zone, New Zealand. Geofluids 4, 259–283.
Rowland, J.V., Baker, E., Ebinger, C.J., Keir, D., Kidane, T., Biggs, J., Hayward, N., Wright, T.J., 2007. Fault growth at a nascent slow-spreading ridge: 2005 Dabbahu rifting episode, Afar. Geophysical Journal International 171, 1226–1246, doi:10.1111/j.1365-246X.2007.03584.x.
Schlische, R.W., Young, S.S., Ackermann, R.V., Gupta, A., 1996. Geometry and scaling relations of a population of very small rift-related faults. Geology 24, 683–686.
Schulz, S.E., Evans, J.P., 1998. Spatial variability in microscopic deformation and composition of the Punchbowl fault, southern California: implications for mechanisms, fluid-rock interaction, and fault morphology. Tectonophysics 295, 223–244.
Secor, D.T., 1965. Role of fluid pressure in jointing. American Journal of Science 265, 633–646.
Sheldon, H.A., Micklethwaite, S., 2007. Damage and permeability around faults: Implications for mineralization. Geology 34, 903–906, doi:10.1130/G23860A.1.
Shipton, Z.K., Cowie, P.A., 2001. Damage zone and slip-surface evolution over μm to km scales in high-porosity Navajo sandstone, Utah. Journal of Structural Geology 23, 1825–1844.
Shipton, Z.K., Evans, J.P., Dockrill, B., Heath, J., Williams, A.P., Kirschner, D., Kolesar, P.T., 2005. Natural leaking CO_2-charged systems as analogs for failed geologic storage reservoirs. In: Thomas, D.C., Benson, S.M. (Eds.), Carbon Dioxide Capture for Storage in Deep Geologic Formations, Vol. 2, pp. 699–712.
Sibson, R.H., 1987. Earthquake rupturing as a mineralizing agent in hydrothermal systems. Geology 15, 701–704.
Simmons, S.F., Browne, P.R.L., 2000. Hydrothermal minerals and precious metals in the Broadlands-Ohaaki Geothermal System: Implications for understanding low-sulfidation epithermal environments. Economic Geology 95, 971–999.
Simmons, S.F., Brown, K.L., 2006. Gold in magmatic hydrothermal solutions and the rapid formation of a giant ore deposit. Science 314, 288–291.
Simmons, S.F., White, N.C., John, D.A., 2006. Geological Characteristics of Epithermal Precious and Base Metal Deposits. Economic Geology 100th Anniversary Volume, 485–522.
Soliva, R., Benedicto, A., 2004. A linkage criterion for segmented normal faults. Journal of Structural Geology 26, 2251–2267, doi:10.1016/j.jsg.2004.06.008.
Talwani, P., Chen, L., Gahalaut, K., 2007. Seismogenic permeability, k_s. Journal of Geophysical Research 112, B07309, doi:10.1029/2006JB004665.
Templeton, D.C., Dreger, D.S., 2006. Non-double-couple earthquakes in the Long Valley volcanic region. Bulletin of the Seismological Society of America 96, 69–79.

Tenthorey, E., Fitz Gerald, J., 2006. Feedbacks between deformation, hydrothermal reaction and permeability evolution in the crust: Experimental insights. Earth and Planetary Science Letters 247, 117–129.
Tenthorey, E., Cox, S.F., Todd, H.F., 2003. Evolution of strength recovery and permeability during fluid-rock reaction in experimental fault zones. Earth and Planetary Science Letters 206, 161–172.
Toda, S., Stein, R.S., Sagiya, T., 2002. Evidence form the AD 2000 Izu Islands earthquake swarm that stressing rate governs seismicity. Nature 419, 58–61.
Waite, G.P., Smith, R.B., 2002. Seismic evidence for fluid migration accompanying subsidence of the Yellowstone caldera. Journal of Geophysical Research 107, no B9, 2177, doi:10.1029/2001JB000586.
Walsh, J.J., Watterson, J., 1988. Dips of normal faults in British Coal Measures and other sedimentary sequences. Journal of the Geological Society of London 145, 859–873.
Walsh, J.J., Watterson, J., 1991. Geometric and kinematic coherence and scale effects in normal fault systems. In: Geological Society, London, Special Publications, vol. 56, pp. 193–203.
Walsh, J.J., Bailey, W.R., Childs, C., Nicol, A., Bonson, C.G., 2003. Formation of segmented normal faults: a 3-D perspective. Journal of Structural Geology 25, 1251–1262.
Watterson, J., Childs, C., Walsh, J.J., 1998. Widening of fault zones by erosion of asperities formed by bed-parallel slip. Geology 26, 71–74.
White, D.E., 1955. Thermal springs and epithermal ore deposits. Economic Geology 50th Anniversary Volume, 392–423.
White, D.E., 1981. Active geothermal systems and hydrothermal ore deposits. Economic Geology 75th Anniversary Volume, 392–423.
White, N.C., Hedenquist, J.W., 1995. Epithermal gold deposits: styles, characteristics, and exploration. Society of Economic Geologists Newsletter 23 1 and 9–13.
Woodcock, N.H., Dickson, J.A.D., Tarasewicz, J.P.T., 2007. Transient permeability and reseal hardening in fault zones: evidence from dilation breccia textures. In: Geological Society, London, Special Publications, vol. 270, 43–53.
Worsley, M.R., Golding, S.D., 1990. Golden Plateau gold deposits. In: Hughes, F.E. (Ed.), Geology of the Mineral Deposits of Australia and Papua New Guinea. The Australasian Institute of Mining and Metallurgy, pp. 1509–1514.